

Stepanenko D.O., Stovpchenko G.P., Togobitskaya D.M., Lisova L.O.

## Evaluating the structural state of fluoride-oxide melts and their interactions with steel to sensible selection of ESR slag

Степаненко Д.О., Стовпченко Г.П., Догобицька Д.М., Лісова Л.О.

### Оцінка структурного стану фтористо-оксидних розплавів для вибору раціонального складу при їх взаємодії зі сталлю в процесі ЕШП

**Purpose.** Evaluation of the structural state of slag melts in the  $\text{CaF}_2\text{-Al}_2\text{O}_3\text{-CaO}$  system with varying contents of  $\text{SiO}_2$  (1; 2.5; 4 wt.%) and  $\text{MgO}$  (3; 6; 12 wt.%), based on their viscosity and electrical conductivity data, for a sensible selection of the optimal chemical composition that will ensure the efficiency of the electroslag process. **Methodology.** Correlation-regression analysis of the relationships between the properties of electroslag remelting slags and their chemical composition and temperature; adaptive segmented linear regression examination of the graphical dependence of the logarithms of viscosity ( $\eta$ ) and electrical conductivity ( $\chi$ ) on temperature ( $\ln(\eta, \chi) = f(1/T)$ ); thermodynamic modelling of the equilibrium composition of metal-slag-gas system phases using HSC Chemistry 9 software. **Scientific novelty.** A new approach is employed to assess the temperature ranges of structural changes induced by alterations in the energy barrier (activation energy) associated with the formation or dissociation of compounds and interactions between different types of ions. The approach is based on the analysis of temperature dependences of structure-sensitive properties (viscosity ( $\eta$ ) and electrical conductivity ( $\chi$ )) using the adaptive segment regression method. **Practical value.** The dependencies of the temperatures of the structural state changes ( $T_1$  – derived from viscosity data,  $T_2$  – derived from electric conductivity) and the intervals between them ( $\Delta T$ ) on the chemical composition of the studied slags can be reliably represented by the parameter  $\rho$  – stoichiometry index (the ratio of cations ( $\text{Ca}^{2+}$ ,  $\text{Mg}^{2+}$ ,  $\text{Si}^{4+}$ ,  $\text{Al}^{3+}$ , etc.) to anions ( $\text{O}^{2-}$ ,  $\text{S}^{2-}$ ,  $\text{F}$  etc.)). The slag composition (wt.%)  $\text{CaF}_2$ – 31,  $\text{Al}_2\text{O}_3$ – 31,  $\text{CaO}$ – 31,  $\text{SiO}_2$ –4,  $\text{MgO}$ –3 provides suitably low values of phase transition temperatures  $T_1 = 1454\text{K}$ ,  $T_2 = 1153\text{K}$  and a wide range between them  $\Delta T = 301\text{K}$  that make it promising for energy effective ESR in short-collar mold with ingot withdrawing.

**Key words:** slag, melt, chemical composition, viscosity, electrical conductivity, temperature, structure, electroslag remelting.

**Мета.** Оцінити структурний стан шлакових розплавів системи  $\text{CaF}_2\text{-Al}_2\text{O}_3\text{-CaO}$  з різним вмістом  $\text{SiO}_2$  (1; 2,5; 4 мас%) і  $\text{MgO}$  (3; 6; 12 мас.%) за даними їх в'язкості та електропровідності для обґрунтованого вибору раціонального складу, що забезпечить ефективність процесу електрошлакового переплаву (ЕШП). **Методика.** Кореляційно-регресійний аналіз зв'язку властивостей шлакових розплавів процесу електрошлакового переплаву з їх хімічним складом та температурою; аналіз графічної залежності логарифмів в'язкості ( $\eta$ ) і електропровідності ( $\chi$ ) від температури ( $\ln(\eta, \chi) = f(1/T)$ ) з використанням методу адаптивної сегментованої лінійної регресії; термодинамічне моделювання рівноважного фазового складу в системі метал-шлак-газ з використанням програмного забезпечення HSC Chemistry 9. **Наукова новизна.** Використано новий підхід до оцінки температурних інтервалів структурних змін, які спричинені зміною енергетичного бар'єру (енергії активації) утворення або дисоціації сполук та взаємодії між різними типами іонів, що відображається на температурних залежностях структурно-чутливих властивостей (в'язкості ( $\eta$ ) та електропровідності ( $\chi$ )) розплавів. **Практична значимість.** Обґрунтовано раціональний склад шлаку для ЕШП з вмістом в ньому компонентів (мас. %):  $\text{CaF}_2$  – 31,  $\text{Al}_2\text{O}_3$  – 31,  $\text{CaO}$  – 31,  $\text{SiO}_2$  – 4,  $\text{MgO}$  – 3, який забезпечує бажані низькі значення температур фазового переходу  $T_1 = 1454\text{K}$ ,  $T_2 = 1153\text{K}$  та широкий інтервал між ними  $\Delta T = 301\text{K}$ . Встановлено зв'язок залежностей значень  $T_1$ ,  $T_2$  та  $\Delta T$  досліджуваних шлаків з їх хімічним складом, представленим параметром  $\rho$  – показник стехіометрії системи, що дорівнює відношенню кількості катіонів ( $\text{Ca}^{2+}$ ,  $\text{Mg}^{2+}$ ,  $\text{Si}^{4+}$ ,  $\text{Al}^{3+}$  та ін.) до аніонів ( $\text{O}^{2-}$ ,  $\text{S}^{2-}$ ,  $\text{F}$  та ін.) з коефіцієнтом детермінації 0,78; 0,95 та 0,86 відповідно.

**Ключові слова:** шлак, розплав, електрошлаковий переплав, в'язкість, електропровідність, температура, структура.

**Introduction.** Research into the physicochemical processes of electroslag remelting (ESR) and various electroslag technologies, invented by B. I. Medovar at the E. O. Paton Electric Welding Institute of the NAS of Ukraine, has surged in recent years due to growing consumer demands for higher-quality ESR metal and the need to enhance production efficiency. The key to the efficiency of

the ESR technological process and the quality of the ingot lies in a well-founded choice of slag composition. A strong current flow generates heat in the slag melt, which is essential for melting and refining the consumable electrode metal from impurities like sulphur and non-metallic inclusions. In addition, the slag forms a thin film (slag skin) between a mould's inner surface and an ingot,

© Степаненко Д.О. – к.т.н., ІЧМ ім Некрасова  
Стовпченко Г.П. – д.т.н., проф., Tianjin Heavy Industry  
research and Development Co, Ltd, Тяньцзінь, Китай  
Тогобицька Д.М. – д.т.н., проф. ІЧМ ім Некрасова  
Лісова Л.О. – к.т.н., Інститут електрозварювання  
ім.Є.О.Патона

© Stepanenko D.O. – Iron and steel institute of Z.I. Nekrasov  
Stovpchenko G.P. – Tianjin Heavy Industry research and  
Development Co, Ltd, Tianjin, China  
Togobitskaya D.M. – Iron and steel institute of Z.I. Nekrasov  
Lisova L.O. – E.O. Paton Electric Welding Institute



This is an Open Access article under the CC BY 4.0  
license <https://creativecommons.org/licenses/by/4.0/>

ensuring its smooth and even surface. Several other requirements for slags are formulated [1-3] depending on the functions that must be ensured when using them in ESR. Ensuring the fluidity of the slag melts at operating temperatures is essential in electroslag remelting processes. The slag must be readily fusible, with its melting point below (from 100 to 500 degrees, according to various estimations) the liquidus temperature of a remelted metal. Usually, the melting of multicomponent slags (except for the eutectic composition) occurs in a certain temperature range caused by structural changes. Two main methods for determining them are thermodynamic calculation and experiment [4-6].

The first method involves determining the equilibrium phase composition of the slag and how it changes depending on temperature, pressure, component concentration, and so on. The results' accuracy depends on the incoming information's reliability and completeness. In actual processes, controlling thermodynamic parameters, such as the partial pressure of gases and their chemical composition, proves challenging, which diminishes the accuracy of calculations and the determination of their melting points. The experimental determination of the melting point (Standard DIN 51730) involves visually observing the alteration in the sample's geometric size as it is heated. Temperatures are recorded while visually detecting the shapes of the sample as defined in the standard. The accuracy of measurements is influenced by subjective factors (such as an experimenter's experience) and objective factors (visually different melting behavior of slags with dissimilar chemical compositions). Moreover, the geometric shape of slag samples usually differs, thereby reducing the repeatability of results due to variations in melting.

**The purpose and objectives of the research.** A new approach was used to estimate the temperature ranges characterizing structural changes in the slag melt of the  $\text{CaF}_2\text{-Al}_2\text{O}_3\text{-CaO-SiO}_2\text{-MgO}$  system. It is based on the approximation of the dependencies  $\ln(\eta, \chi) = f(1/T)$  [7], using the adaptive segmented linear regression method and the modelling of linear segments (temperature ranges), where the activation energies of viscosity ( $E_\eta$ ) and electrical conductivity ( $E_\chi$ ) are independent of temperature. The fulfilment of the condition  $E_\eta, E_\chi \neq f(T)$  serves as evidence for the constancy of the melt structure; alterations in their values across different temperature ranges indicate a change in the structure [8-11].

The temperature stability intervals of the melt structure, as well as the temperatures at which changes in structural state occur, were determined based on the experimental data of viscosity and electrical conductivity of  $\text{CaF}_2\text{-Al}_2\text{O}_3\text{-CaO}$  slags with varying contents of  $\text{SiO}_2$  (1; 2.5; 4 wt.%) and  $\text{MgO}$  (3; 6; 12 wt.%) [12] to justify the rational composition of the slag. The equilibrium content of the components of the gas-slag-metal system (under the

technological conditions of electroslag remelting of Cr11MoV steel at PJSC Dnipropetsstal) was calculated to support the informed selection of ESR slag.

**Research results.** It is known that the physicochemical properties of slag melt, particularly viscosity and electrical conductivity, depend on the chemical composition and temperature, reflecting structural changes in a melt [13-17]. According to contemporary concepts [13], viscosity is determined by the content and type of polymer-forming anions, specifically  $\text{Si}_x\text{O}_y^{z-}$ ,  $\text{Al}_x\text{O}_y^{z-}$ , and electrical conductivity more depend on the mobile cations ( $\text{Ca}^{2+}$ ,  $\text{Mg}^{2+}$ ,  $\text{O}^-$ ,  $\text{F}^-$  etc.) concentrations. The basic equations for the mathematical description of the temperature dependence of viscosity ( $\eta$ ) and electrical conductivity ( $\chi$ ) are expressions (1) and (2), accordingly, proposed by J. Frenkel [18].

$$\eta = A \cdot e^{\frac{E_\eta}{RT}}, \quad (1)$$

$$\chi = B \cdot e^{-\frac{E_\chi}{RT}}, \quad (2)$$

where: T – the absolute temperature (K); A and B – constants; R – the universal gas constant (8.314·J/(mol K));  $E_\eta$  and  $E_\chi$  are the activation energies of viscosity and electrical conductivity (J/mol), accordingly.

Formulas (1) and (2) illustrate the exponential dependence of the reaction rate constant on temperature, as the fundamental Arrhenius equation describes. According to these fundamental principles, the logarithmic relationships of viscosity ( $\ln(\eta)$ ) and electrical conductivity ( $\ln(\chi)$ ) concerning temperature ( $1/T$ ) are valid under the following conditions:

$$A, B, E_\eta, E_\chi \neq f(T). \quad (3)$$

The viscosity of most slag melts deviates from the Arrhenius equation, as its activation energy changes inversely proportional with temperature increasing [15, 19-21]. Such a change in activation energy with temperature permits slag melts to be classified as structurally heterogeneous liquids exhibiting various types of chemical bonds between ions. Similar to the viscosity of slag melts, the deviation from condition (3) is similarly maintained for the temperature ( $1/T$ ) dependence of the logarithm of electrical conductivity. Determining the temperature ranges at which condition (3) for  $\ln(\eta, \chi) = f(1/T)$  will be satisfied holds both theoretical and practical significance for exploring the composition-structure-properties relationship of slag melts. To model the specified temperature ranges for ESR slags of the  $\text{CaF}_2\text{-Al}_2\text{O}_3\text{-CaO-SiO}_2\text{-MgO}$  system (Table 1), the relevant values of viscosity (Fig. 1) and electrical conductivity (Fig. 2) were involved based on the experimental data of [12].

Table 1 – Chemical composition of slags in calculation

Slag Number	Content of components, wt. %				
	CaF <sub>2</sub>	Al <sub>2</sub> O <sub>3</sub>	CaO	MgO	SiO <sub>2</sub>
1	31	31	31	3	4
2	31.5	31	32	3	2.5
1	32	32	32	3	1
4	31	31	31	6	1
5	29	29	29	12	1

The adaptive segmented linear regression method [7] was applied for calculations of the linear sections of the temperature dependences  $\ln(\eta) = f(1/T)$ ,  $\ln(\chi) = f(1/T)$  based on the experimental data on viscosity and electrical conductivity (Figs. 1

and 2) of the investigated slags. The temperatures of structural transitions  $T_1$  and  $T_2$  (Fig. 3, 4, and Table 2) were calculated and plotted against the original data for viscosity and electrical conductivity in Figures 1 and 2, respectively.

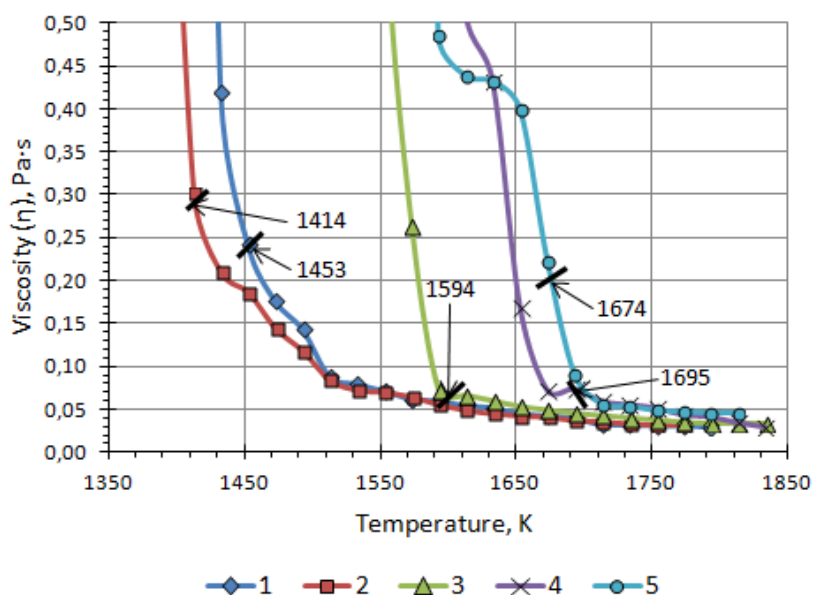


Figure 1 – Temperature dependence of slag viscosity (Table 1) [12]. Marks on the graphs are temperatures of structural transitions  $T_1$  (Figs. 3, 4, and Table 2).

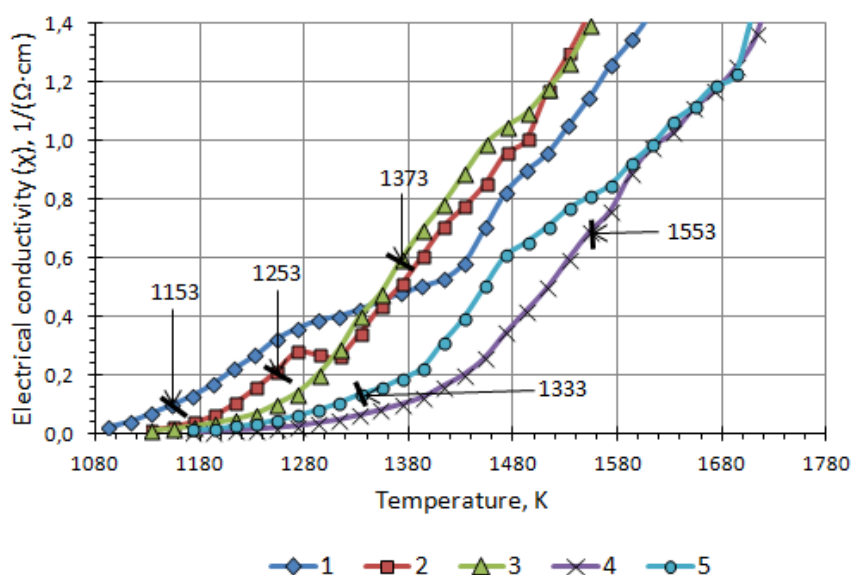


Figure 2 – Temperature dependence of slag electrical conductivity (Table 1) [12]. Marks on the graphs are temperatures of structural transitions  $T_2$  (Figs. 3, 4, and Table 2).

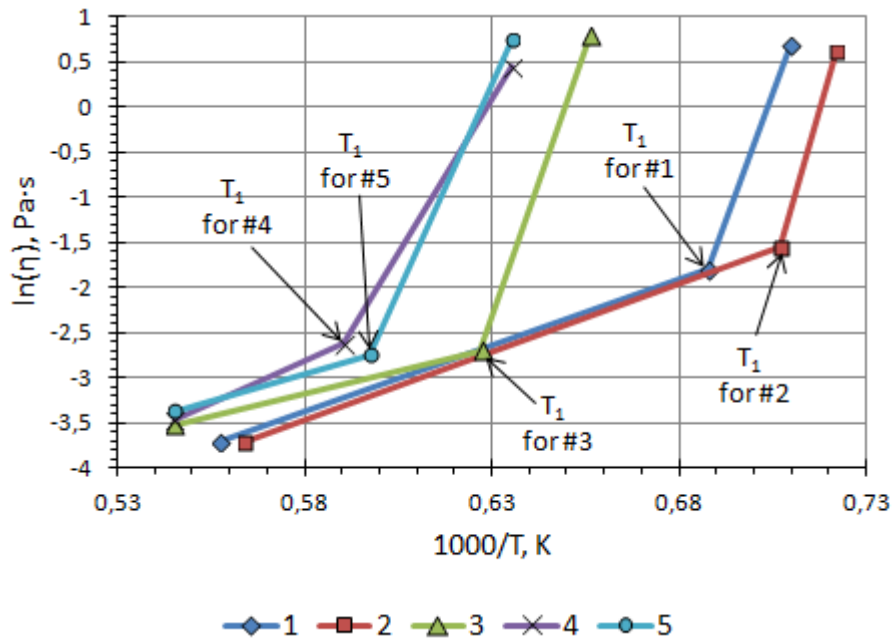


Figure 3 – Linear sections of temperature dependences of the logarithms of viscosity ( $\ln(\eta)$ ) of slags (numbering according to Table 1).

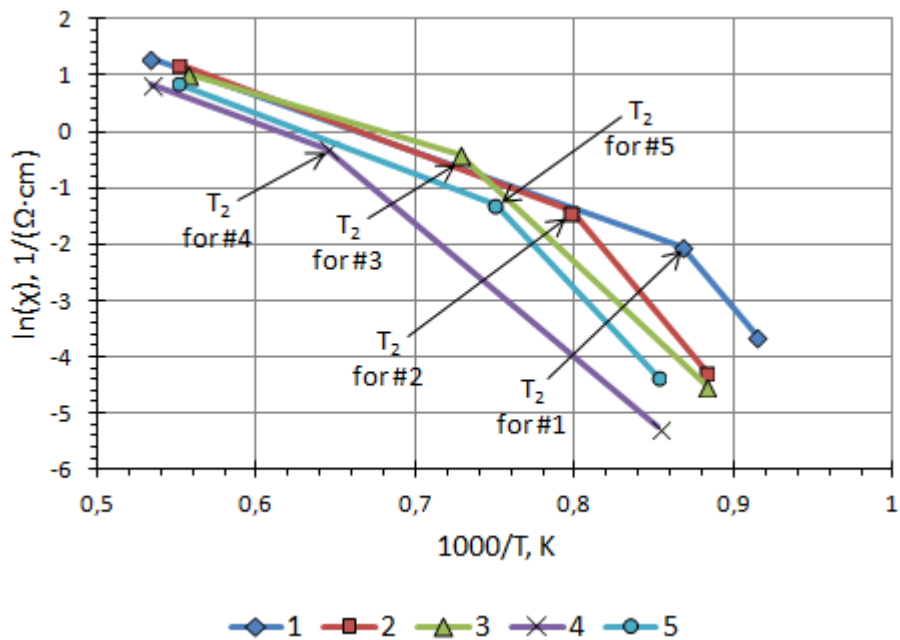


Figure 4 – Linear sections of temperature dependences of the logarithms of electrical conductivity ( $\ln(\chi)$ ) of slags (numbering according to Table 1).

From the calculation results (Fig. 3 and 4) it is evident that  $\ln(\eta, \chi) = f(1/T)$  dependencies have high-temperature and low-temperature linear sections with particular values of temperature intervals. The consistency of activation energies and structure are characteristic of these linear sections. The temperatures that are common to the high-temperature and low-temperature sections for both  $\ln(\eta) = f(1/T)$  (designation  $T_1$  in Fig. 3) and  $\ln(\chi) = f(1/T)$  (designation  $T_2$  in Fig. 4) have

theoretical and practical value. The corresponding values of  $T_1$  and  $T_2$  and the difference between them ( $\Delta T$ ) are presented in Table 2.

Figures 5 and 6 illustrate the graphical relationships of the values of  $T_1$ ,  $T_2$ , and  $\Delta T$  for the studied slags in relation to their chemical composition, represented by the parameter  $\rho$  - an indicator of the stoichiometry of a system, which means the ratio of cations ( $\text{Ca}^{2+}$ ,  $\text{Mg}^{2+}$ ,  $\text{Si}^{4+}$ ,  $\text{Al}^{3+}$ , etc.) to anions ( $\text{O}^-$ ,  $\text{S}^{2-}$ ,  $\text{F}^-$ , etc.) [22].

Table 2 – Temperatures  $T_1$  and  $T_2$  received by the adaptive segmented linear regression method from dependencies  $\ln(\eta, \chi) = f(1/T)$

Slag Number	$\rho$	$T_1$ , K	$T_2$ , K	$\Delta T$ , K
1	0,688	1454	1153	301
2	0,694	1414	1253	161
3	0,697	1594	1373	221
4	0,706	1695	1553	142
5	0,725	1674	1333	341

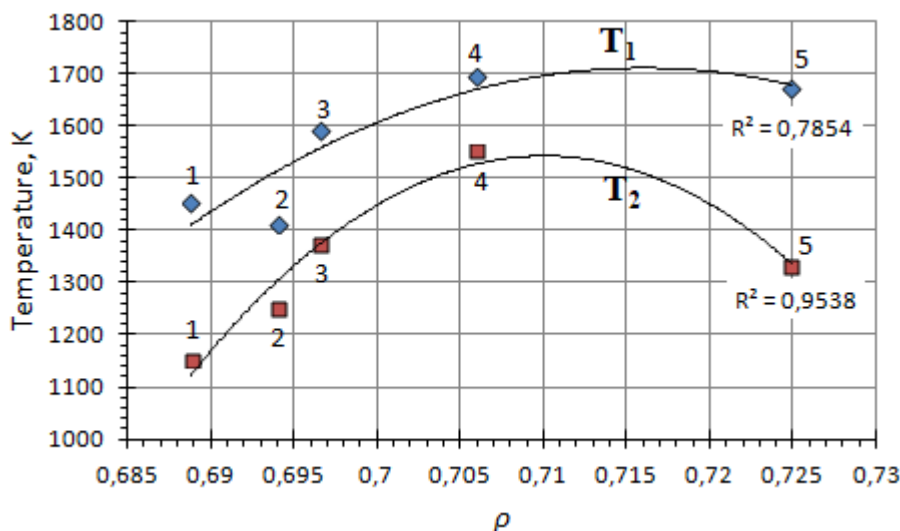


Figure 5 – Dependence of temperatures  $T_1$  and  $T_2$  on the slag stoichiometry index –  $\rho$ . The numbers on the graphs correspond to the slags listed in Table 2.

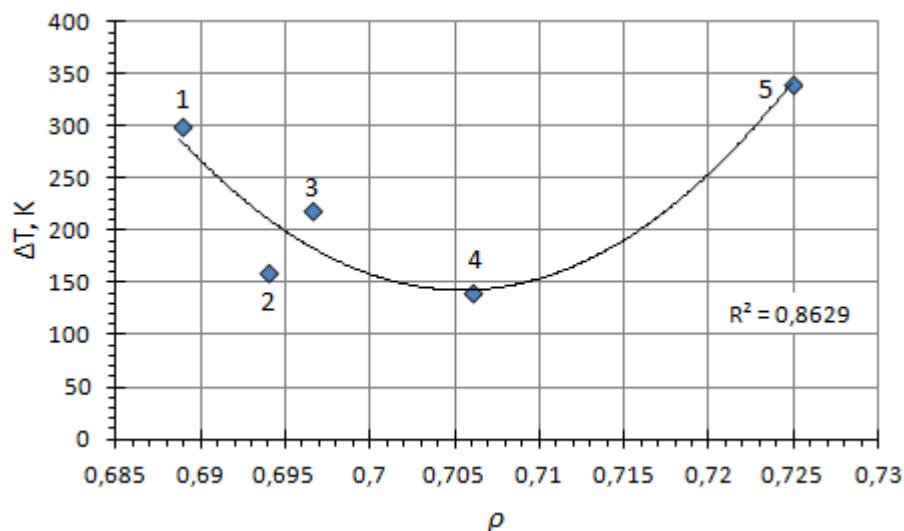


Figure 6 – Dependence of  $\Delta T$  as the difference between  $T_1$  and  $T_2$  on the slag stoichiometry index -  $\rho$ . The numbers on the graphs correspond to the slags listed in Table 2.

It is shown that slag #1 (Tables 1, 2) has the lowest phase transition temperatures  $T_1 = 1454$  K,  $T_2 = 1153$  K and a wide range between them  $\Delta T = 301$  K, making it a good candidate for ESR in view of the above-substantiated requirements specified above.

Thermodynamic calculations. Using the HSC Chemistry 9 software, the equilibrium compositions for the thermodynamic gas-slag-metal system were calculated during electroslag remelting of Cr11MoV steel (Table 3) under slags (Table 1) in an inert gas atmosphere (argon) and a temperature of 1873 K [12].

Table 3 – Chemical composition of steel Cr11MoV, which is accepted in calculations

Component	C	Si	Mn	Cr	Mo	V	Cu	Ni	S
Content, wt. %	0,15	0,5	0,7	11	0,7	0,3	0,3	0,3	0,025

It is accepted that the specific consumption of slag is 44 kg per ton of metal (ingot 4300 kg in weight). Thermodynamic calculations of the equilibrium content of the components of the gas-slag-metal system have shown that the content of

active components of the slag and metal phases is subject to significant changes (Table 4). They are redistributed between the phases (the initial values (before interaction) and final (after it) ones are shown in Figures 7-11).

Table 4 – Equilibrium content of the most active and variable components of the slag, gas, and metal phases at 1873 K.

Slag Number	Content of components, wt.%					
	Metal		Gas		Slag	
	Si	Al	CO	Mn	MnO	FeO
1	0,494	0,019	0,28	0,06	0,04	0,01
2	0,500	0,012	0,37	0,07	0,06	0,01
3	0,503	0,009	0,46	0,04	0,07	0,02
4	0,494	0,019	0,27	0,05	0,04	0,01
5	0,495	0,018	0,27	0,05	0,05	0,01

The formation of MnO and FeO oxides in the equilibrium composition indicates the slag's oxidising effect on the metal. A sign of this is also the

oxidation of aluminium, which is accompanied by an increase in the Al<sub>2</sub>O<sub>3</sub> content in the slag (Fig. 7) and is minimal for slags #1 and #4.

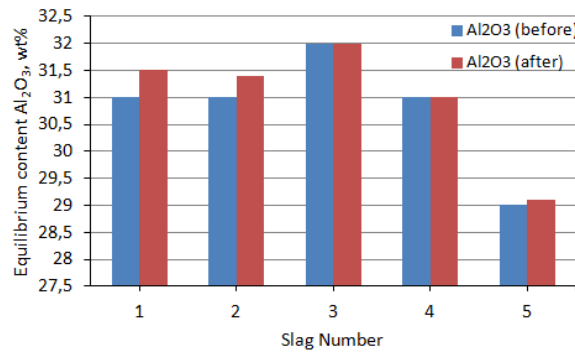


Figure 7 – Comparison of initial (before interaction between slag and metal) and final (after it) Al<sub>2</sub>O<sub>3</sub> content.

The most remarkable oxidation of aluminium is associated with increased SiO<sub>2</sub> content (slags #2 and #3). Increased MgO content within the studied limits has almost no effect. A decrease in the CaO

content in the equilibrium composition occurs for all slags, which may be associated with calcium sulfide formation, promoting metal desulfurization (Fig. 8).

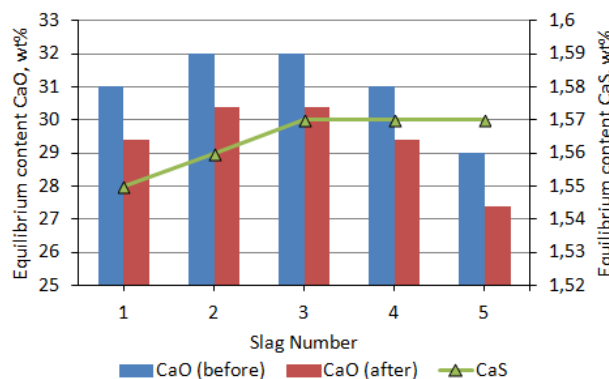


Figure 8 – Change in the content of CaO and CaS in the slag phase.

The highest amount of CaS compound (1.57 wt.%) is shown for systems with slags #1, #4, and #5, which indicates that the increase in magnesium content from 3 to 12 wt.% does not affect the

formation of sulfides. The desulfurization capacity of the slag decreases with an increase in the silica content from 1 to 4 wt.%.



Insignificant evaporation of magnesium and decreased MgO content in the slag are also predicted (Fig. 9).

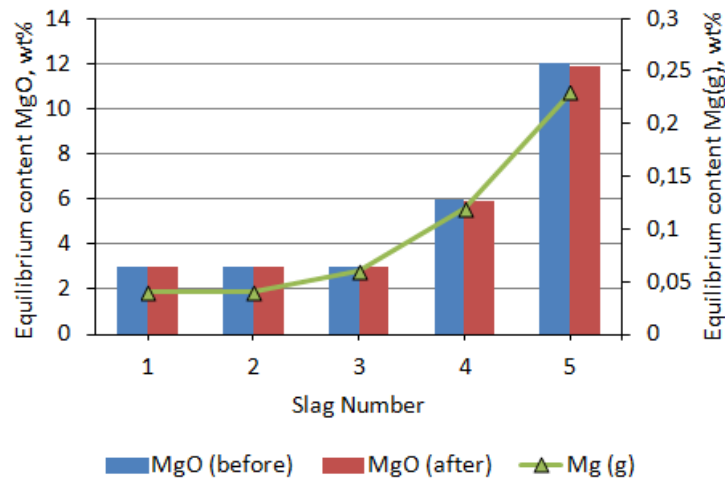


Figure 9 – Change in MgO content in slag and Mg vapor content in the gas phase.

It should be noted that increasing the SiO<sub>2</sub> content to 4 wt.% with a constant MgO content (3 wt.%) reduces its evaporation to the gas phase (the lowest value is 0.04 wt.% for slag #3). The

formation of CaF<sub>2</sub> vapors in the gas phase is also predicted, which naturally decreases with the lowering of its content in the slags (Fig. 10).

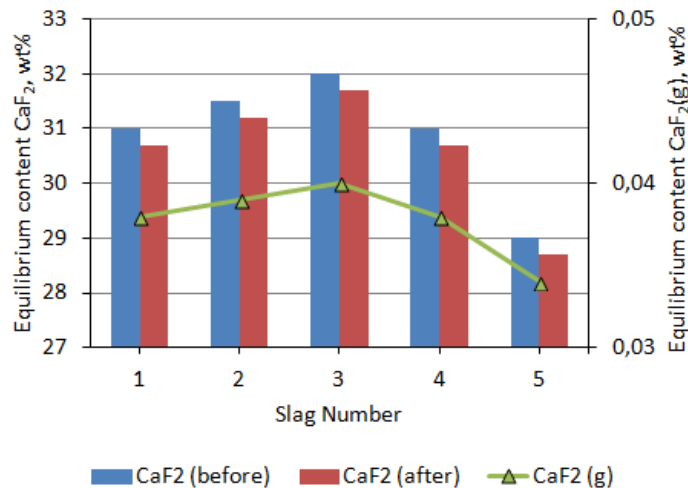


Figure 10 - Change in CaF<sub>2</sub> content and its evaporation.

The use of all slag compositions with 1 wt.% SiO<sub>2</sub> demonstrated negligible oxidation of silicon from the metal composition. With a slag content of 2.5 wt.% SiO<sub>2</sub>, the silicon content in the metal and silicon oxide in the slag remain nearly at the initial level (Fig. 11). With a content of 4 wt.% SiO<sub>2</sub>, there is an insignificant reduction of silicon in the metal observed.

The equilibrium chromium content in steel has remained almost unchanged, and the amount of chromium oxide in the slag phase is insignificant. The highest value of  $3.4$  to  $3.7 \times 10^{-5}$  wt.% is predicted for slag #3, while the minimum is for slags #1 and #5 ( $4$  to  $8 \times 10^{-6}$  wt.% and  $5$  to  $7 \times 10^{-6}$  wt.%, respectively). Thermodynamic calculations have demonstrated the fundamental feasibility of using all the studied slags from the

CaF<sub>2</sub>-Al<sub>2</sub>O<sub>3</sub>-CaO-SiO<sub>2</sub>-MgO system for remelting Cr11MoV steel while maintaining the original composition within acceptable limits.

The results were validated by the pilot industrial test at Dniprospeksstal [23] involving the electroslag remelting of ingots (565×565 mm, 4300 kg) made from high-alloy steel Cr11MoV, which also demonstrated full compliance with standard requirements. In comparison to the slag ANF-6 (70 % CaF<sub>2</sub>, 30 % Al<sub>2</sub>O<sub>3</sub>) utilized at Dniprospeksstal, there was a reduction in metal contamination with oxide ribbon non-metallic inclusions by 0.5 points, an increase in relative elongation by 12.5 %, and a decrease in energy consumption by 17 % resulting from the lower electrical conductivity of the proposed slag.

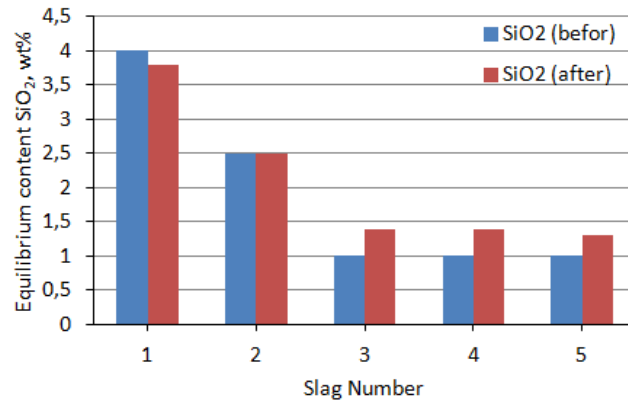


Figure 11 – Change in SiO<sub>2</sub> content in the slag phase

By employing a new method to evaluate the structure of slag melts, the composition of slag #1 is marked as exhibiting low structural transition temperatures (based on the viscosity and electrical conductivity temperature curves) alongside a broad interval between the phase transformation points. This slag is promising for ESR with a short-collar mold, where the long-term presence of liquid slag with an unaltered structure is crucial for achieving a smooth ingot surface. The researched slags of the CaF<sub>2</sub>-Al<sub>2</sub>O<sub>3</sub>-CaO-SiO<sub>2</sub>-MgO system are recommended as a replacement for ANF-6 slag in the electroslag remelting of high-alloy steels to enhance energy efficiency and reduce costs, owing to the twofold lower content of calcium fluoride.

### Conclusions

A new approach for estimating the temperatures of structural state changes in slag melts based on approximating the adaptive segmented linear regression of  $\ln(\eta, \chi) = f(1/T)$  dependencies and modelling linear segments (temperature intervals) in which the activation energies of viscosity ( $E_\eta$ ) and electrical conductivity ( $E_\chi$ ) are unrelated of temperature was applied.

The temperatures of the structural state changes ( $T_1$  and  $T_2$ ), along with the interval between them ( $\Delta T$ ), were determined based on experimental data

on the viscosity and electrical conductivity of ESR slags from the CaF<sub>2</sub>-CaO-Al<sub>2</sub>O<sub>3</sub> system, which contains SiO<sub>2</sub> (1; 2.5; 4 wt.%) and MgO (3; 6; 12 wt.%).

The relationships between structural changes and the composition of the studied slags were identified using the stoichiometry indicator  $\rho$  (the ratio of cations (Ca<sup>2+</sup>, Mg<sup>2+</sup>, Si<sup>4+</sup>, Al<sup>3+</sup>, etc.) to anions (O<sup>2-</sup>, S<sup>2-</sup>, F<sup>-</sup>, etc.)), which describes the dependencies of  $T_1$ ,  $T_2$ , and  $\Delta T$  values on the chemical composition of slags, with determination coefficients of 0.78, 0.95, and 0.86, respectively.

The slag containing (wt.%) CaF<sub>2</sub>- 31, Al<sub>2</sub>O<sub>3</sub>- 31, CaO- 31, SiO<sub>2</sub>-4, MgO-3 is promising to facilitate the smooth ingot surface formation in short-collar mold ESR, due to providing the suitably low values of phase transition temperatures  $T_1 = 1454$  K,  $T_2 = 1153$  K, and the wide range between them  $\Delta T = 301$  K.

Thermodynamic calculation shows that additions of SiO<sub>2</sub> affect the properties of studied slags much more than MgO. Increasing SiO<sub>2</sub> from 1 to 4 wt.% in the studied system results in metal component oxidation, diminishes MgO evaporation from slags, and reduces their desulphurization ability.

### References

1. Medovar, L. B., Stovpchenko, A. P., Lisova, L. A., Dzhyanh, Dzh. (2012). Sovremennue trebovaniya k protsessam y shlakam elektroshlakovoho pereplava. *Metallurhicheskaia i hornorudnaia promushlennost*, (7), 297-301
2. Medovar, B. Y. et al. (1988) *Elektroshlakovaia tyhelnaia plavka i razlyvka metalla* [Paton B. E. (Ed.)]. Naukova Dumka
3. Stovpchenko, G. P., Lisova, L. O., Goncharov, I. O., & Gusiev, I. V. (2018). Physico-chemical properties of the ESR slags system CaF<sub>2</sub>-Al<sub>2</sub>O<sub>3</sub>-(MgO, TiO<sub>2</sub>). *Journal of Achievements in Materials and Manufacturing Engineering*, 89 (2), 64-72. <https://doi.org/10.5604/01.3001.0012.7110>
4. Guo, C., Shang, S., Du, Z., Jablonski, P. D., Gao, M. C., & Liu, Z.-K. (2015). Thermodynamic modeling of the CaO-CaF<sub>2</sub>-Al<sub>2</sub>O<sub>3</sub> system aided by first-principles calculations. *Calphad*, 48, 113-122. <https://doi.org/10.1016/j.calphad.2014.12.002>
5. Ju, J., Gu, Y., Zhang, Q., & He, K. (2023). Effect of CaF<sub>2</sub> and CaO/Al<sub>2</sub>O<sub>3</sub> ratio on evaporation and melting characteristics of low-fluoride CaF<sub>2</sub>-CaO-Al<sub>2</sub>O<sub>3</sub>-MgO-TiO<sub>2</sub> slag for electroslag remelting. *Ironmaking & Steelmaking*, 50(1),13-20. <https://doi.org/10.1080/03019233.2022.2079938>



6. Hou, D., Pan, P., Wang, D., Hu, S., Wang, H., & Zhang, G. (2021). Study on the Melting Temperature of CaF<sub>2</sub>-CaO-MgO-Al<sub>2</sub>O<sub>3</sub>-TiO<sub>2</sub> Slag under the Condition of a Fixed Ratio of Titanium and Aluminum in the Steel during the Electroslag Remelting Process. *Materials*, 14, 6047. <https://doi.org/10.3390/ma14206047>
7. Togobytska, N., Stepanenko, D., & Möhs, C. (2023). Adaptive segmented regression for the modeling of temperature-dependent material properties. *22nd ECMI Conference on Industrial and Applied Mathematics*. 23-30 June 2023 – Wrocław, Poland, 327. <https://ecmi2023.org/book-of-abstracts>
8. Kwack, T., Um, H., & Chung, Y. (2023). Activation Energy of Alumina Dissolution in FeO-Bearing Slags. *Metals*, 13, 1702. <https://doi.org/10.3390/met13101702>
9. Yang, D., Zhou, H., Wang, J., et al. (2021). Influence of TiO<sub>2</sub> on viscosity, phase composition and structure of chromium-containing high-titanium blast furnace slag. *Journal of Materials Research and Technology*, 12, 1615-1622. <https://doi.org/10.1016/j.jmrt.2021.03.069>
10. Li, T., Sun, C., Song, S., & Wang, Q. (2019). Influences of Al<sub>2</sub>O<sub>3</sub> and TiO<sub>2</sub> Content on Viscosity and Structure of CaO-8%MgO-Al<sub>2</sub>O<sub>3</sub>-SiO<sub>2</sub>-TiO<sub>2</sub>-5%FeO Blast Furnace Primary Slag. *Metals*, 9, 743. <https://doi.org/10.3390/met9070743>
11. Sajid, M., Bai, C., Aamir, M., et al. (2019). Understanding the Structure and Structural Effects on the Properties of Blast Furnace Slag (BFS). *ISIJ International*, 59(7), 1153-1166. <https://doi.org/10.2355/isijinternational.ISIJINT-2018-453>
12. Lisova, L. O., Stovpchenko, G. P., Goncharov, I. O. et al. (2020). Thermodynamics of interaction and physical properties of 30CaF<sub>2</sub>/30CaO/30Al<sub>2</sub>O<sub>3</sub> system slags with addition of SiO<sub>2</sub> and MgO in different ratios in electroslag remelting. *Suchasna elektrometalurgiya*, 1, 8-13. <https://doi.org/10.37434/sem2020.01.01>
13. Min, D. J., & Tsukihashi, F. (2017). Recent advances in understanding physical properties of metallurgical slags. *Met. Mater. Int.* 23, 1–19. <https://doi.org/10.1007/s12540-017-6750-5>
14. Stepanenko, D. A., Volkova, O., Heller, H. P. et al. (2017). Selecting optimal slag conditions in the blast furnace. *Steel Transl.*, 47, 610–613. <https://doi.org/10.3103/S0967091217090133>
15. Stepanenko D. (2023). Calculation of activation energy of viscosity for evaluation of metallurgical slag melts structure. *Lithuanian Journal of Physics*, 63(1), 40-45. <https://doi.org/10.3952/physics.2023.63.1.6>
16. Stovpchenko, G., Togobitskaya, D., Lisova, L., Stepanenko, D., & Medovar, L. (2022). Predictive models for molten slags viscosity and electrical conductivity based on directed chemical bonds concept. *Ironmak. Steelmak.*, 49(6), 572–580. <https://doi.org/10.1080/03019233.2022.2026043>
17. Zhang, L., Jiang, K., Xie, F., & Lu, D. (2023). Relation between Viscosity and Conductivity of CaO-MgO-FeO-Al<sub>2</sub>O<sub>3</sub>-SiO<sub>2</sub> System for Copper Smelting Slags. *Metals*, 13, 786. <https://doi.org/10.3390/met13040786>
18. Frenkel, Ya. Y. (1975). *Kynetycheskaia teoriia zhydkostei*. Nauka
19. Sukenaga, S., Gueguen, Y., Celarie, F., et al. (2024). Effect of calcium and potassium oxide addition on the viscosity and fragility of a calcium aluminosilicate melt. *Journal of the American Ceramic Society*, 107(6), 3822-3836. <https://doi.org/10.1111/jace.19722>
20. Hunt, A. G. (2000). Fragility of liquids using percolation-based transport theories: Correlation between limiting slope of the viscosity and non-exponentiality of relaxation. *Journal of Non-Crystalline Solids*, 274(1–3), 93-101. [https://doi.org/10.1016/S0022-3093\(00\)00206-4](https://doi.org/10.1016/S0022-3093(00)00206-4)
21. Nascimento, M. L. F., & Aparicio, C. (2007). Viscosity of strong and fragile glass-forming liquids investigated by means of principal component analysis. *Journal of Physics and Chemistry of Solids*, 68(1), 104-110. <https://doi.org/10.1016/j.jpcs.2006.09.013>
22. Prykhodko, E. V., Tohobytskaia, D. N., Khamkhotko, A. F., & Stepanenko, D. A. (2013). *Prohnozyrovanye fizyko-khymycheskykh svoistv oksyduh system*. Porohy
23. Stovpchenko, H. P., Davydchenko, S. V., Lisova, L. O., Husiev, Ya. V., & Medovar, L. B. (2020). Doslidzhennia tekhnolohichnosti ta efektyvnosti novoho shlaku dlia elektroshlakovoho pereplavu. *Suchasna elektrometalurhiia*, (3), 11-17. <https://doi.org/10.37434/sem2020.03.01>

Надійшла до редколегії / Received by the editorial board: 28.08.2023  
Прийнята до друку / Accepted for publication: 20.11.2023